

Adaptive oncology phase I trial design of drug combinations with drug-drug interaction modeling

YANG YANG*, HONG-BIN FANG, ANINDYA ROY, AND MING TAN*

The goal of a Phase I trial is to find the maximum tolerated dose (MTD). In a single-agent dose finding Phase I trial, the key underlying assumption is that toxicity probability increases monotonically with the dose level. However, in multi-agent trials, this assumption may not hold because the drug-drug interaction potentially can either decrease or increase the joint toxicity as compared to either one used alone, which may lead to an unforeseen toxicity probability surface. Thus there exists multiple MTDs. We first develop a novel adaptive dose-finding approach which can be applied to these kinds of multi-drug combination trials. With this approach, drug-drug interaction and toxicity probability are modeled jointly through a Bliss independence model. The main goal of our dose finding scheme is to search for *maximum tolerated region* (MTR), as opposed to maximum tolerated dose (MTD), in single agent phase I trials. The method allows exploration of more combinations in the phase I stage, which is of particular relevance in oncology since phase I trials on the combinations may be the only opportunity before launching a costly phase III trial, comparing selected combination(s) with a standard of care. Dose escalation/de-escalation decision rules are determined by the posterior estimates of both joint toxicity probability and the corresponding drug-drug interaction, which can be continuously updated by sequentially assigning new patients into the trial while more data is being observed. We evaluate the operating characteristics of the proposed method through extensive simulation studies under various scenarios. The proposed method demonstrates satisfactory performance. In addition, the MTR offers several combinations that investigators may choose to advance to future trials based on external information from e.g., preclinical antitumor activities and other trials.

KEYWORDS AND PHRASES: Adaptive Bayesian design, Bliss independence, Drug combination, Dose finding, Interaction index function, Maximum tolerated dose (MTD), Maximum tolerated region, Objective function.

1. INTRODUCTION

The purpose of a Phase I clinical trial of a single-agent is to find the maximum tolerated dose (MTD), which is a dose

with acceptable dose-limiting toxicity (DLT) level (probability). There is a large amount of literature on phase I trial designs [31, 32, 34], which can be classified largely into two categories: rule-based methods and model-based methods. Rule-based methods, such as the 3+3 design, assign the next cohort of patients using prespecified dose escalation (or deescalation) rules, given whether toxicity is present or not in the previous cohort. As an alternative to the rule-based design, a model-based approach utilizes all data accumulated at a given time during the trial to model the dose-toxicity curve, and estimate a dose that will have the prespecified targeted probability of dose-limiting toxicity. For instance, the continual reassessment method (CRM), or its variants [19, 30, 31] based on Bayesian updating of a dose response/toxicity model, are most widely used in practice. In anti-cancer drug development, combination therapy is very important due to drug resistance in monotherapy. Thus it is no surprise that in recent years, cancer therapeutics have focused on combinations of two or more agents in both pre-clinical and clinical trials. Such developments present unusual challenges to clinical trial design. In single agent trials, the toxicity probability is often assumed to increase monotonically with the dose level, resulting in a simple order of toxicity probability. Contrarily, the toxicity order in two-dimensional dose combination space is usually unknown due to potential interaction in toxicity between the two drugs. There exists multiple MTDs. Furthermore, because of their potential synergistic interactions in efficacy, the high dose combinations of two drugs may not result in better efficacy (for example, see Fang et al. [13]). Synergistic interaction in terms of toxicity can also occur, thus the low dose combinations of two drugs may not always have less toxicity. The issues of drug-drug interaction in finding MTD of two drug combinations are summarized well in Korn and Simon [21]: “consideration should therefore be given to more precisely defining the MTD in combination phase I trials”. The dose combinations with the potential for greater effect and less toxicity will be desired in the consequent phase II trial.

Over the last two decades, in response to the need for an ever increasing number of combination studies, several model based statistical designs have been developed for dose-findings with two or more agents in Phase I trials. Simon and Korn [33] suggested a graphical method called “tolerable dose diagram” to search an optimal combination region based on “total equivalent dose”. Thall et al. [40] proposed a model based two-stage Bayesian design for the trial

*Corresponding authors.

of gemcitabine and cyclophosphamide. Like one-dimensional CRM, dose combinations were first escalated along the diagonal direction in their two-dimensional dose region until the maximum sample size of stage 1 is reached. Then two additional treatment combinations were identified based on a toxicity equivalence contour. Wang and Ivanova [44] proposed a Bayesian design where they used a 3-parameter model for the toxicity probabilities of the dose combination with two cytotoxic agents given together. They fixed the level of one agent and varied the dose level of the other. Then the two-dimensional dose-finding trial was converted into a group of one-dimensional dose finding subtrials, and the MTD was identified in each sub trial. Yin and Yuan [46] developed a latent contingency table approach for the combined agents. In their two-dimensional dose space, the doses were allowed to be escalated and deescalated “non-diagonal” toward a dose combination with acceptable toxicity. Subsequently, Yin and Yuan [45] proposed another Clayton-copula type regression model to link the joint toxicity probability with marginal probability. More recently, Wages et al. [42] laid out the partial orderings of toxicity probabilities across the treatment combinations, using CRM to estimate MTDs along these orders.

Different from single agent trials, the interaction between two agents may have significant impact on the joint toxicity probability of the dose combination. The different states of interactions are generally described as being independent, synergistic or antagonistic. The independence model implies that the two drugs have no apparent interaction with respect to toxicity. Synergy occurs when the combined agents exhibit greater toxicity than when they act independently. Antagonism refers to the situation where one drug reduces or neutralizes the toxicity of another [5, 17]. In the majority of existing dose-finding methods for combined agents, monotonicity of toxicity is assumed [40, 44, 45, 46, 47]. It says that, the joint toxicity probability is increasing with doses of either agent. Underneath this assumption, it is assumed that only synergistic and independent effects take place between the agents uniformly for all situations where the monotonicity is assumed. However, the biochemical and biological effects of the combined agents are complex. Antagonism can also happen, where the joint toxicity probability may decrease when one agent is added to another. This is rarely the case in practice, but we usually do not know the direction of the interaction when designing a trial on drug combination. More importantly, it is not reasonable to assume that the interaction in toxicities is consistent over all combinations in the experimental dose region. The interaction of synergy or antagonism may vary with the different dose combinations in the two-dimensional space, which may also lead to non-monotonicity of the dose-toxicity curve. As a specific motivating example, consider a phase 1 combination study of Neratinib and Temezirolimus for treating metastatic solid tumors [16, 26]. For example, if we fix Temezirolimus at the dose level 15 (mg), the observed DLT rates at dose levels of (15, 120), (15, 160), (15, 200) and (15, 240) are calculated

as 0%, 12%, 0% and 50%, respectively. Although the combination of Neratinib with Temezirolimus shows substantial synergistic tumor growth inhibition in preclinical studies, we do not know how the two drugs will interact in terms of toxicity. If emerging toxicity and dose data can be utilized sequentially to update the two-drug interaction pattern and the dose response surface, the dose escalating scheme can be expected to be more efficient.

To address these issues, we develop a new joint model for toxicity and interaction in clinical setting utilizing insight from preclinical drug interaction modeling [15, 36] to define the interaction. We propose to use the Bliss model to evaluate the binary toxicity outcome of combination therapy of two agents and also incorporate an interaction function to detect different patterns of synergy, independence or antagonism across the combinations. We assume a parametric model for the toxicity probability $g(\mathbf{x}, \boldsymbol{\theta})$, as a function of the dose \mathbf{x} and a parameter vector $\boldsymbol{\theta}$, and define a *maximum tolerated region* (MTR), which consists of the doses that have the toxicity probabilities below the target toxicity probability ϕ ,

$$(1) \quad MTR = \{\mathbf{x} : g(\mathbf{x}, \boldsymbol{\theta}) \leq \phi\}.$$

Our primary goal is to determine the MTR. We propose a Bayesian scheme in which we will estimate MTR as $\widehat{MTR} = \{\mathbf{x} : E\{g(\mathbf{x}, \boldsymbol{\theta})|\text{data}\} \leq \phi\}$ where the expectation is taken with respect to the posterior of $\boldsymbol{\theta}$. The factors, such as the efficiency of dose escalation process and ethical requirements of the toxicity level staying within pre-specified level, are also incorporated into our considerations. Our solution is to search a dose-allocation path in the two-dimensional space with a trade-off between toxicity and interaction that provides efficient estimation of MTR while locating the assignment to the least synergistic dose combinations. As the trial proceeds, we sequentially update the posterior estimates of the interaction effects and the toxicity surface. At each stage, the patient cohort allocated to the next dose is determined by taking into consideration the available toxicity and interaction effect estimates. At the end of the trial, based on the preclinical data in vivo and in vitro [13], one or more doses in the MTR may be selected for subsequent trials. Selection of a bag of potential candidates, i.e., the combinations belonging to the MTR, separates the procedure from those which select a single MTD in the multi-agent trial. The selection of a set of drug combinations offers a useful alternative and provides more flexibility for the choice of drug combinations to be used in Phase II. Recognizing the complexity of the problem, the final recommendations may be derived based on synthesizing information from the phase I data, external preclinical, and clinical data, and even from adding expansion cohorts of patients for the MTDs selected in the Phase I protocol.

The remainder of the article is organized as follows. In Section 2, we introduce a novel Bliss model to evaluate the toxicity probability and the interaction effect. In Section 3, we describe a dose allocation algorithm that applies to this

model. In section 4, we conduct extensive simulation studies to examine the operating characteristics of the proposed method under various scenarios. Finally, we conclude with a discussion on the characteristics of the proposed approach and potential extensions.

2. TOXICITY PROBABILITY MODEL AND PARAMETRIC ESTIMATION

In order to predict the toxicity response to a drug combination, it is important to characterize the nature of the drug interaction. Loewe additivity and Bliss independence, recommended by the Saariselka agreement [1, 3], are two commonly used reference models for no interaction. The Loewe additivity defines zero interaction by equation

$$(2) \quad d_A/D_A + d_B/D_B = 1.$$

where (d_A, d_B) is the combination dose-level of agents A and B, which produces an effect E , and D_A and D_B are the doses of agents A and B which produce the same magnitude of the effect E , when either agent is given alone. The Loewe additivity model is based on the assumption that a drug has no interaction by itself and is used to assess the efficacy of drug combinations. Under the Bliss independence model, the expected effect of a combination of two agents can be calculated from the single-agent effects $E_A(d_A)$, $E_B(d_B)$ by

$$(3) \quad E_{(AB)} = E_A + E_B + E_A E_B.$$

Let $P(A)$ and $P(B)$ be the marginal toxicity probabilities of agents A and B, respectively. If agent A and agent B are independent, the probability of no toxicity in the combination of A and B is

$$(4) \quad 1 - P(A \cup B) = \{1 - P(A)\}\{1 - P(B)\}.$$

Thus, the joint toxicity probability of the agents is $1 - \{1 - P(A)\}\{1 - P(B)\}$. Clearly, for the binary toxicity outcome, the Bliss independence model is more appropriate as a reference model for identifying the interaction effects than Loewe additivity. For dose levels d_A for agent A and d_B for agent B, the joint probability of toxicity has the form

$$(5) \quad g(d_A, d_B) = 1 - \{1 - g(d_A, 0)\}\{1 - g(0, d_B)\},$$

where $g(d_A, 0)$ and $g(0, d_B)$ are the marginal toxicity probabilities of agents A and B, respectively. Then Bliss toxicity synergy is defined as

$$(6) \quad g(d_A, d_B) > 1 - \{1 - g(d_A, 0)\}\{1 - g(0, d_B)\}.$$

For Bliss antagonism, the inequality is reversed. The Bliss antagonism results in more lowering toxicity at a given drug combination than that expected under Bliss independence. To specify the toxicity response $g(d_A, d_B)$, several parametric models have been proposed in the literature. For example, Yin and Yuan proposed both Clayton-copula and

Gumbel-copula models [45, 46]. However, the existing models are not able to describe dose response patterns when some combination doses are synergistic while other combinations doses are independent or antagonistic. To overcome this limitation, we propose a factorial type Bliss model that allows mixed interaction profiles for the combination therapy using agents A and B on the binary toxicity outcome. The probability of toxicity is modeled as follows:

$$(7) \quad g(d_A, d_B, \boldsymbol{\theta}) = 1 - [\exp(-\alpha d_A - \beta d_B)]^{f(\gamma_1, \gamma_2, d_A, d_B)},$$

where $\alpha > 0$, $\beta > 0$ and γ_1, γ_2 are parameters to be estimated. The function $f(\gamma_1, \gamma_2, d_A, d_B)$ is used to measure the degree of synergy or antagonism of the different dose combinations. We propose using the following form

$$(8) \quad f(\gamma_1, \gamma_2, d_A, d_B) = \exp(-d_A d_B (\gamma_1 d_A + \gamma_2 d_B)).$$

The model satisfies the conditions that if $d_B = 0$, then $g(d_A, 0) = 1 - \exp(-\alpha d_A)$. This is the toxicity model of single drug A. Similarly, when $d_A = 0$, then $g(0, d_B) = 1 - \exp(-\beta d_B)$ and the toxicity model reduces to that of the single drug B. Thus, the implied single drug toxicity models are the conventional exponential toxicity models that assume a monotonically increasing dose-toxicity model at each margin. The proposed model captures antagonism when $f(\gamma_1, \gamma_2, d_A, d_B) < 1$, independence when $f(\gamma_1, \gamma_2, d_A, d_B) = 1$ and synergy when $f(\gamma_1, \gamma_2, d_A, d_B) > 1$. Hence, we call $f(\gamma_1, \gamma_2, d_A, d_B)$ the interaction function.

To estimate parameters $\alpha, \beta, \gamma_1, \gamma_2$, we adopt a Bayesian approach. Without loss of generality, we rescale the dose space to $[0, 1]^2$ and specify the model based on the rescaled doses. One of the reasons for rescaling is for numerical stability of the Bayesian computation scheme. Let $0 \leq a_1 < \dots < a_I < 1$ be the specific dose levels of drug A and $0 \leq b_1 < \dots < b_J < 1$ be the specific dose levels of drug B. Suppose n_{ij} patient received the dose combinations (a_i, b_j) . Denote $y_{ijm} = 1$ if the m -th patient at dose level (a_i, b_j) experienced toxicity, otherwise, $y_{ijm} = 0$. Assume that dose allocation and the associated toxicity data from the first $n_L = \sum_{i,j=1}^L n_{ij}$ patients, $\Omega_L = \{(a_1, b_1, y_{1,1,1}), \dots, (a_1, b_1, y_{1,1,n_{11}}), \dots, (a_L, b_L, y_{L,L,n_{LL}})\}$ are available. The likelihood of the unknown parameter vector is given by

$$(9) \quad L(\boldsymbol{\theta}) \propto \prod_{i,j=1}^L \prod_{m=1}^{n_{ij}} [g(a_i, b_j, \boldsymbol{\theta})]^{y_{ijm}} [1 - g(a_i, b_j, \boldsymbol{\theta})]^{1 - y_{ijm}}.$$

In this nonlinear model, estimates of nonlinear parameters may be highly correlated with each other, especially when covariates themselves are correlated [25]. This ‘‘ill-conditioning’’ may cause difficulty in estimating parameters simultaneously. Thus, we use informative priors for parameters α and β , which may be estimated based on either the

historical data from previous single agent trials or elicitation of expert opinion. We will assume that the parameters α and β follow a gamma distribution $\pi_1(\alpha) = \pi_1(\beta) = \text{Gamma}(\nu_1, \nu_2)$ since α and β are positive. The results with different prior parameters ν_1 and ν_2 are similar for overall performance as shown in Table 5b below. Parameters (γ_1, γ_2) are assigned vague priors with $\pi_2(\gamma_1) = \pi_2(\gamma_2) = N(\eta_1, \eta_2)$. We center the prior mean η_1 at 0 with a relatively large variance. For our specific case, we choose the variance η_2 to be 100. The prior distributions of the model parameters are taken to be independent. The posterior density of $\theta = (\alpha, \beta, \gamma_1, \gamma_2)$ is given by

$$(10) \quad H(\theta|\Omega_L) \propto L(\Omega_L|\theta)\pi(\theta),$$

where $\pi(\theta) = \pi_1(\alpha)\pi_1(\beta)\pi_2(\gamma_1)\pi_2(\gamma_2)$. The posterior distributions of the unknown parameters are computed using Markov chain Monte Carlo (MCMC) algorithm. The first crucial step is to use the posterior mode estimate as an initial starting point. Let the logarithm of the posterior density be,

$$(11) \quad h(\theta|\Omega_L) = \log(H(\theta|\Omega_L)).$$

We denote the posterior mode θ by $\hat{\theta}$. Using the Laplace approximation, θ can be approximated as:

$$(12) \quad \theta \sim MVN(\hat{\theta}, (-h''(\hat{\theta}))^{-1}).$$

The posterior mode θ is found by maximizing posterior $h(\theta)$ using the Nelder-Mead algorithm [29]. In addition, in order to construct a proposal distribution, we also compute the variance-covariance matrix $(-h''(\hat{\theta}))^{-1}$ evaluated at $\hat{\theta}$. The posterior density is simulated by alternate use of a random walk proposal and an independence chain [18]. We start the simulation with initial state $\theta = \hat{\theta}$. The independence chain uses a proposal based on an $MVN(\hat{\theta}, \hat{\Sigma})$ approximation to the joint posterior distribution. Specifically, given $\theta^{(s)}$, to generate the sample $\theta^{(s+1)}$ joint posterior distribution, the Metropolis algorithm is summarized as follows:

1. Sample $\theta^* \sim MVN(\theta^s, (-h''(\theta^s))^{-1})$.
2. Compute the acceptance ratio $r = \frac{h(\theta^*|\Omega_L)}{h(\theta^s|\Omega_L)}$.
3. Sample $u \sim \text{uniform}(0, 1)$; set $\theta^{s+1} = \theta^*$ if $u < r$ and $\theta^{s+1} = \theta^s$ otherwise.

We run 5,000 iterations of the Metropolis independence chain but discard the first 1000 draws. The toxicity probability is evaluated at the each iteration. The estimated posterior toxicity probability $p(\hat{\theta})$ is calculated by averaging all these toxicity probabilities. We evaluate the model performances by using this sampling scheme and present the percentage of interaction functions, identifying the true synergy or antagonism in Web Appendix A.

3. DOSE FINDING ALGORITHM

In this section, we propose a method to find the maximum MTR for a given target probability. The method integrates

the toxicity interaction of the two drugs and the Bayesian adaptive dose-finding algorithm. The primary goal of the algorithm is to determine the shape of the MTR. At the same time, because therapeutic benefit always exists at higher doses, it is desirable to bring more patients to higher doses, while restricting the escalation to the MTR. To incorporate this feature, our next step is choosing the next dose combination \mathbf{x}_{n+1} from the potential escalation set E_t to find the dose combination which has the smallest posterior mean toxicity, such as $\mathbf{x}_{n+1} = \arg \min_{\mathbf{x} \in E_t} E\{\pi(\mathbf{x}, \theta)|\text{data}\}$. This ap-

proach has the benefit of allowing the design to explore more area in the MTR dose space. For example, within a two-dimensional dose-finding trial, a number of dose combinations among the escalation dose set have an estimated probability of toxicity within the MTR as marked in Figure 1. Let, at stage t , the current dose combination be $(a_t, b_t) \equiv (a, b)$. Our allocation scheme defines the potential escalation set as $E_t = \{(a_t^-, b_t^+), (a_t, b_t^+), (a_t^+, b_t^+), (a_t^+, b_t), (a_t^+, b_t^-)\}$ and the potential de-escalation set as $D_t = \{(a_t^-, b_t^+), (a_t^-, b_t), (a_t^-, b_t^-), (a_t, b_t^-), (a_t^+, b_t^-)\}$. Then the dose with posterior mean probability of DLT closest to the target toxicity probability ϕ is chosen for cohort $n + 1$, that is $\mathbf{x}_{n+1} = \arg \min_{x \in E_t} \{E\{\pi(x, \theta)|\text{data}\} - \phi\}$, as commonly used in many

single agent dose-finding designs [35]. Then the next cohort (referring to Figure 1) are treated at combination (a_t, b_t^+) ; trial would stop as it almost reaches the boundary of MTR. However, this allocation of doses means that little data has been acquired about the toxicity when high doses of drug A are given. Choosing the dose combination with the smallest toxicity probability is likely to prolong the escalation to the higher doses in the hope of learning more about the MTR. This feature differentiates the proposed design from other escalation methods where the goal is to reach the MTD in the quickest way possible. Since we are interested in the entire MTR, and not just a dose combination on the boundary of the region, we devise a method that is better suited for exploration of the dose region. Another goal is to bring the trial to dose combinations that have the least synergistic toxicity so that the patients can be safely assigned to a relatively high dose of individual drugs, which otherwise would not have been possible for a single drug scenario. Thus, patients can be exposed to doses with potentially greater efficacy without experiencing significant toxicity. Our strategy is to incorporate both toxicity probability and interaction function into a single objective function. To stabilize the computation, we rescale the range of the interaction function to $[0, 1]$ to match the range of the probability function. Let $d_A \in \{a_1, \dots, a_I\}$ and $d_B \in \{b_1, \dots, b_J\}$. For given dose levels of agent A at d_A and agent B at d_B , the rescaled interaction function can be defined as:

$$(13) \quad v(d_A, d_B) = \frac{f(\gamma_1, \gamma_2, d_A, d_B)}{f(\gamma_1, \gamma_2, d_A, d_B) + 1}.$$

The goal is to locate a dose combination by minimizing a combination of the interaction function $v(d_A, d_B)$ and the

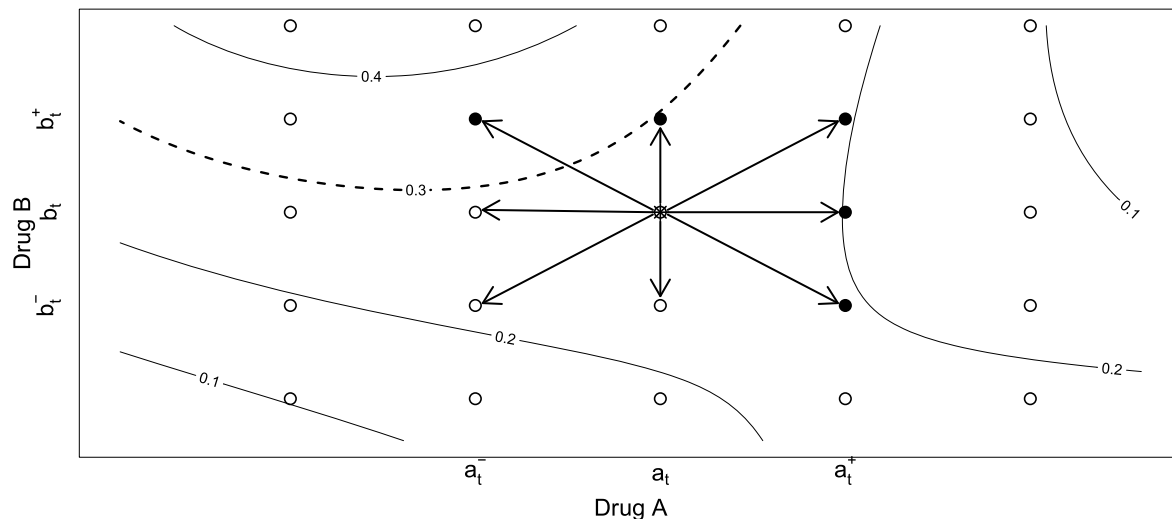


Figure 1. Dose escalation and de-escalation diagram with 5×5 combinations. It also illustrates a next dose combination chosen in a typical case. Suppose the current dose is treated at (a_t, b_t) , represented by a circle enclosing a star. The potential escalation dose set is represented by a shaded circle. The target toxicity probability contour at 0.3 is considered to be the boundary of MTR region.

toxicity probability $g(d_A, d_B)$, subject to the constraint that the toxicity probability is no more than a pre-specified value. We define the objective as a convex combination of the probability of toxicity at dose (d_A, d_B) and the interaction $v(d_A, d_B)$ at that dose. The choice of λ reflects how much emphasis one would like to put on having more allocation at antagonistic combinations.

$$(14) \quad U_\lambda(d_A, d_B) = \lambda g(d_A, d_B) + (1 - \lambda)v(d_A, d_B).$$

where $0 < \lambda \leq 1$. Toxicity probability and interaction function are considered jointly through the objective function with the relative contribution of each component controlled by the weight λ . Smaller values of U would indicate smaller values of the standardized interaction leading to less synergy and smaller toxicity probability. Therefore, the Bayesian adaptive dose-finding design developed also minimizes the objective function. The next dose combination may be chosen to minimize the posterior expectation of the objective function given the current data \mathbf{z}_n ,

$$(15) \quad \mathbf{x}_{n+1} = \arg \min_{\mathbf{x}} \{U_\lambda(\mathbf{x}, \boldsymbol{\theta}) | \mathbf{z}_n\}.$$

In most adaptive design schemes, involving tuning parameters, reasonable values of the tuning parameters are determined through external validation. We conduct extensive empirical studies to evaluate possible λ values over several plausible scenarios in Web Appendix B. We define a performance measure for the adaptive algorithm as a function of λ and optimize the measure over possible values of λ to glean insight into an acceptable range of values for the parameter. Based on our investigation, as reported in the Appendix, a “base case” when $\lambda = 0.5$ is recommended.

Before we describe our main algorithm, we define some notation. For any dose a for drug A, define a^- and a^+ as the doses immediately preceding and immediately following a , respectively, in the sequence of chosen doses. Similarly define b^- and b^+ for dose b of drug B. We denote π_t as the posterior estimate of the toxicity probability surface at stage t . Let ϕ be the target toxicity probability in the trial, and c_s, c_e, c_e and c_d be some prespecified threshold probabilities. We initiate the algorithm at the lowest dose levels of the two agents.

1. The first cohort of patients is treated at the starting dose combination (a_1, b_1) .
2. Subsequently, two other cohorts of patients are escalated to the dose levels (a_1, b_2) and (a_2, b_1) , respectively.

Based on the collected data from (a_1, b_1) , (a_1, b_2) , (a_2, b_1) , we estimate the objective function for (a_1, b_3) , (a_2, b_2) , (a_3, b_1) . Moreover, to constrain the doses to be escalated only within the MTR, we also examine whether the predictive toxicity probabilities of (a_1, b_3) , (a_2, b_2) , (a_3, b_1) , denoted by π_E , satisfy,

$$(16) \quad Pr(\pi_E \leq \phi) > c_s.$$

The dose pair that meets this condition and also has the smallest posterior expectation of the objective function is chosen as the next combination $(a_s, b_{s'})$ where $s, s' > 1$. Because the posterior estimates are often quite unstable at the initial stage, if we cannot find the next dose pair that satisfies condition (16), we would repeat the initiation procedure. If there is still no suitable dose pair, the trial would be terminated for safety.

Our scheme allows the escalation or de-escalation in five directions to increase its adaptability to the shape of the surface, as illustrated in Figure 1. Although monotonic toxicity is not assumed, from a conservative point of view, our design still deescalates the trial if the toxicity is high. In our method, each escalation or de-escalation step is restricted by one level of change.

After these initial steps, the rest of the trial proceeds according to the allocation scheme described in the following:

At stage t , the following algorithm is used to select (a_{t+1}, b_{t+1}) or to decide termination of the trial.

1. If the toxicity probability at the current dose combination (a_t, b_t) , denoted by π_t , satisfies

$$(17) \quad Pr(\pi_t \leq \phi) > c_e,$$

we will consider escalating the dose to the potential escalation set E_t . To constrain the doses to be escalated only within the MTR, we further examine whether the predictive toxicity probabilities of at least one of the potential combinations E_t , denoted by π_{E_t} , satisfy

$$(18) \quad Pr(\pi_{E_t} \leq \phi) > c,$$

and select (a_{t+1}, b_{t+1}) to have the smallest value of the objective $U(a_{t+1}, b_{t+1})$ in the subset of E_t , satisfying (18). If there is no suitable next point, the trial would be terminated.

2. If the toxicity probability at the current dose combination,

$$(19) \quad Pr(\pi_t > \phi) \geq c_d,$$

we will examine whether at least one of the predictive toxicity probabilities of the potential adjacent de-escalated set D_t , denoted by π_{D_t} , satisfies

$$(20) \quad Pr(\pi_{D_t} \leq \phi) > c,$$

and select (a_{t+1}, b_{t+1}) to have the smallest value of the objective in the subset of D_t satisfying (20). If there is no suitable next point, the trial would be terminated.

3. If the toxicity probability at the current dose combination,

$$(21) \quad Pr(\pi_t > \phi) > c_t,$$

The trial will be terminated.

4. Otherwise, the next cohort of patients will be allocated at the current dose.
5. The trial continues until the maximum sample size is reached. Once the trial is terminated, the dose combinations that have toxicity probabilities less than the target ϕ are selected as the MTR combinations.

There are several thresholds involved in the algorithm. The values of c, c_s, c_e, c_d, c_t are typically prespecified. The overall performance of the algorithm is expected to be a function of the values of the thresholds. We use the same values

and similar rationale for setting threshold as previously discussed in Yin and Yuan's algorithm [46]. The c_e and c_d are used to control the rate of escalation or de-escalation; the c, c_s and c_t are chosen to avoid the intensive toxicity. As with other algorithms with pre-specified parameters, the optimal range of values for each threshold can only be determined through full scale external validation. Some thresholds may have natural bounds beyond which values will be deemed unreasonable. Others may need extensive simulation studies for understanding the operating characteristics of the algorithm as a function of the values of those thresholds. We have performed limited simulation studies and have recommended some values for the thresholds that were not found in Yin and Yuan's algorithm. What we have relied on is a qualitative understanding (e.g. high/low) of desirable range of values for each threshold. However, a full scale sensitivity study is still warranted for fully understanding the limits of the performance of the proposed algorithm as a function of the thresholds.

4. SIMULATION STUDY

We examine the performance of the proposed dose-finding algorithm for two-agent combinations under 10 toxicity scenarios as listed in Table 1. The scenarios are constructed to imitate real trial data where toxicity probability surfaces have various shapes in the dose combination space. In the simulations, we first consider the selection probability for the MTR combinations, since the goal of Phase I combination study is to find the MTR. In other side, the misclassification rate of MTR selection is also considered (The false positive rate is the proportion of combination doses outside MTR that are incorrectly classified as MTR dose combinations. The false negative rate is the proportion of MTR dose combinations that are incorrectly classified as combination doses outside MTR.). Furthermore, a sensitivity analysis of different prior selections for parameters is conducted.

We illustrate the first four scenarios in terms of the contours of constant toxicity probability in Figure 2. They represent the agent combination trials with different patterns of the MTR, in which each agent has five dose levels. We specify the dose levels of agent A $(a_1, a_2, a_3, a_4, a_5)$ as $(0.125, 0.25, 0.375, 0.5, 0.625)$, and the dose levels of agent B $(b_1, b_2, b_3, b_4, b_5)$ as $(0.1, 0.3, 0.5, 0.7, 0.9)$. Scenarios 5–10 consider the toxicity surfaces to be monotonically increased. Specifically, Scenarios 5–8 were originally examined by Yin and Yuan using their contingency table design [46], whereas Scenarios 9–10 were examined in their copula regression design [45]. In similar settings, we assume the maximum sample size is 60 patients with a cohort size of 3 and the target toxicity probabilities of $\phi = 30\%$ for scenarios 1–8 and $\phi = 40\%$ for Scenarios 9–10, respectively. The threshold values used in dose escalation and trial termination are also specified accordingly. We use the same threshold values as in

Table 1. Toxicity scenarios for the two-drug combinations. The target MTR combinations are in boldface

Dose Level	Drug A									
	1	2	3	4	5	1	2	3	4	5
	Scenario 1					Scenario 2				
5	0.45	0.48	0.44	0.33	0.20	0.21	0.14	0.12	0.13	0.17
4	0.36	0.38	0.34	0.28	0.21	0.23	0.21	0.22	0.27	0.39
3	0.27	0.30	0.28	0.25	0.22	0.22	0.25	0.30	0.39	0.55
2	0.19	0.22	0.23	0.23	0.19	0.18	0.23	0.30	0.41	0.55
1	0.11	0.16	0.19	0.22	0.26	0.11	0.17	0.23	0.30	0.39
	Scenario 3					Scenario 4				
5	0.35	0.38	0.41	0.56	0.78	0.36	0.33	0.29	0.26	0.25
4	0.30	0.36	0.43	0.58	0.79	0.32	0.32	0.33	0.29	0.28
3	0.26	0.33	0.40	0.54	0.72	0.26	0.28	0.29	0.30	0.35
2	0.19	0.25	0.33	0.44	0.58	0.19	0.23	0.26	0.28	0.29
1	0.11	0.17	0.23	0.30	0.37	0.11	0.16	0.21	0.25	0.27
	Scenario 5					Scenario 6				
4	0.50	0.55	0.60	0.70		0.30	0.50	0.55	0.60	
3	0.15	0.30	0.50	0.60		0.12	0.30	0.50	0.55	
2	0.10	0.12	0.30	0.45		0.10	0.15	0.30	0.45	
1	0.06	0.08	0.10	0.15		0.08	0.12	0.16	0.18	
	Scenario 7					Scenario 8				
3	0.15	0.30	0.50	0.55	0.60	0.50	0.60	0.70	0.80	0.90
2	0.12	0.16	0.30	0.50	0.55	0.10	0.30	0.50	0.70	0.80
1	0.06	0.08	0.10	0.30	0.50	0.06	0.10	0.15	0.30	0.50
	Scenario 9					Scenario 10				
4	0.54	0.67	0.75	0.81	0.86	0.49	0.58	0.68	0.75	0.81
3	0.48	0.59	0.68	0.75	0.81	0.40	0.49	0.59	0.68	0.75
2	0.40	0.45	0.59	0.67	0.74	0.27	0.40	0.45	0.59	0.67
1	0.24	0.40	0.47	0.56	0.64	0.18	0.29	0.40	0.47	0.56

Yin and Yuan’s algorithm; $c_e = 0.7, c_d = 0.45$ for Scenarios 1–8 and $c_e = 0.8, c_d = 0.45$ for Scenarios 9–10. We set $c_s = 0.55, c = 0.7, c_t = 0.9$, and simulate 2000 trials under each scenario. Moreover, instead of generating toxicity probabilities from our model, we choose the toxicity probabilities arbitrarily to demonstrate robustness of the proposed design.

Table 2 presents the selection probabilities for the MTR combinations under Scenarios 1–4, and also reports the numbers of patients treated at each dose combination averaged over 2000 simulations in those 4 scenarios. The boundary of MTR under Scenario 1 is a U-shaped contour for target toxicity probability at 0.3, whereas the boundary contour under Scenario 2 is in C-shape. Both scenarios are designed to examine whether the proposed method would allocate patients into the MTR, as the toxicity probability may not increase in either the vertical or the horizontal directions. Our proposed procedure is able to select the MTR dose combinations with higher frequency compared to the ones outside the MTR. At least 86% of patients have been allocated into the MTR under both scenarios. The MTR in Scenario 3 is located at the lower left-hand corner of the two-dimensional space. Our design identifies the MTR in the correct position and stops the trial earlier before a large number of patients are treated at toxic doses. Scenario 4 is the most complex case with an x-shaped boundary. Typically escalation al-

gorithms will have difficulty in identifying such MTR. Our method still allocates the patients into the MTR with high percentages. Although our method selects some dose combinations outside the MTR with relatively high percentages, it is expected, given that their toxicity contours are very close to the boundary.

Table 3 reports the selection probabilities for the MTR combinations and the numbers of patients treated across each dose combination under Scenarios 5–10, in which the toxicity surfaces are monotonically increasing as MTDs are considered to be on the boundary of the MTRs. It implies that our proposed procedure is able to select the MTR dose combinations with higher frequency compared to the ones outside the MTR in all the scenarios, even in cases when the proposed method performs less well. For instance, under scenario 8, our method allocates a relatively large portion of patients to the doses outside MTR, such as the doses (a_1, b_3) and (a_2, b_3) . However, in terms of correctly selecting the MTR, the proposed design yields a higher percentage for the doses inside the MTR when compared with the ones outside. We compare the percentage of observed toxicities and the percentage of patients treated at or below the MTDs between the proposed method and the two designs of Yin [45, 46]. In terms of the percentage of observed toxicities, the designs of Yin and Yuan only gain slightly

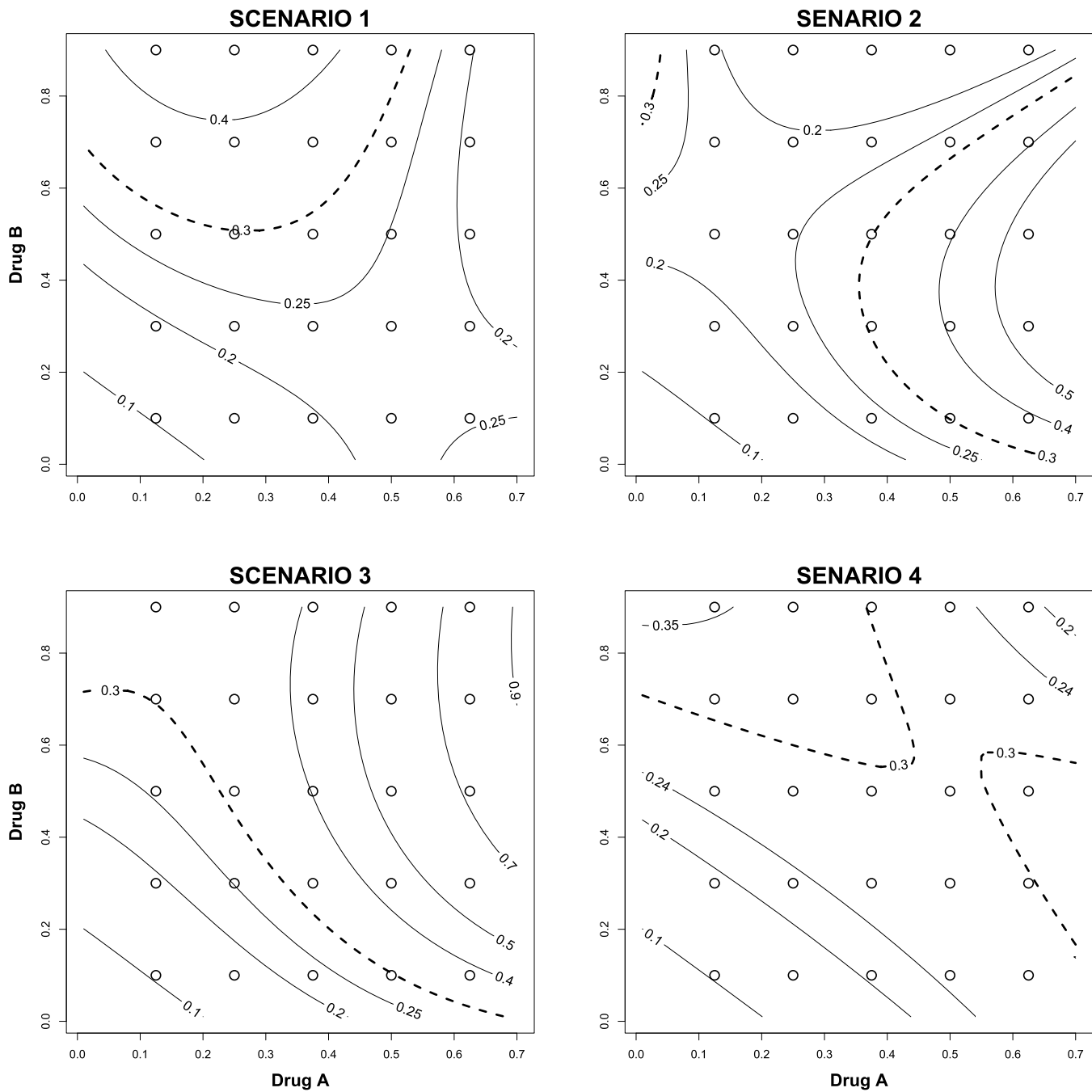


Figure 2. Scenarios for the probability of toxicity as a function of Drug A and B doses in combination trial. The target toxicity probability contour at 0.3 is considered to be the boundary of MTR region.

in performance with a smaller percentage of observed toxicities in Scenario 9. However, in Scenarios 5, 6, 7, 8 and 10, our method improves upon the performance of Yin and Yuan considerably in each case. The proposed design also performs well in locating patients at the doses under the target toxicity probability. In Scenarios 5, 6, 7, 9 and 10, our method improves the percentage of patients under or below the MTDs, at least 4% higher than those with the

Yin and Yuan's method. Our method performs worse under scenario 8 since the movements of our design might be constrained when the dose levels of two drugs are quite imbalanced. However, the performance of our method could be improved by using more stringent thresholds. The simulation results indicate that the overall performance of the new method is satisfactory and it offers an attractive alternative to the existing two-dimensional dose-finding methods. Fur-

Table 2. Percentage of MTR selection and number of patients treated at each dose combination under scenarios 1–4; the target MTR combinations are in boldface

Dose Level	Drug A										
	Percentage of MTR Selection					Number of Patients Allocation					
	1	2	3	4	5	1	2	3	4	5	
Drug B	Scenario 1					Scenario 1					
	5	7.1	5.1	4.4	4.5	10.5	0.15	0.21	0.07	0.04	0.29
	4	9.1	4.5	4.4	10.5	12.3	0.38	0.33	0.05	0.36	0.19
	3	19.7	7.2	11.5	14.1	14.3	1.42	0.01	0.89	0.04	0.39
	2	82.2	33.1	24.1	20.2	20.3	4.82	1.79	0.07	0.33	0.64
	1	99.9	98.5	62.6	41.8	33.3	3.85	4.94	2.56	1.04	0.32
	Scenario 2					Scenario 2					
	5	21.1	20.0	16.4	12.4	15.2	0.27	0.55	0.47	0.31	0.39
	4	23.3	18.7	12.6	13.4	12.9	0.50	0.46	0.02	0.31	0.04
	3	32.0	17.9	13.9	12.7	8.8	1.49	0.03	0.77	0.03	0.06
	2	84.0	32.0	17.3	10.5	9.2	4.56	1.65	0.07	0.28	0.25
	1	99.9	98.6	55.3	30.1	20.2	3.82	4.80	2.52	0.89	0.24
	Scenario 3					Scenario 3					
	5	9.8	6.8	3.8	1.7	2.5	0.25	0.32	0.16	0.04	0.06
	4	12.2	5.2	1.9	2.8	3.7	0.42	0.41	0.06	0.18	0.01
	3	22.0	5.2	3.9	4.7	3.9	1.55	0.01	0.78	0.03	0.05
	2	81.2	26.3	10.7	7.1	6.2	5.03	1.91	0.09	0.26	0.29
	1	99.9	98.3	55.9	29.8	19.4	3.87	5.24	2.71	0.96	0.27
	Scenario 4					Scenario 4					
	5	11.4	8.8	6.4	5.2	10.1	0.25	0.36	0.18	0.10	0.27
4	14.0	7.9	5.4	10.2	10.7	0.42	0.41	0.04	0.37	0.12	
3	24.2	10.4	11.5	11.4	10.1	1.44	0.01	0.85	0.05	0.26	
2	82.9	31.4	20.0	15.3	15.0	4.84	1.62	0.05	0.32	0.54	
1	99.9	98.3	59.7	37.3	28.4	3.83	5.03	2.56	0.96	0.32	

ther details regarding results of the alternative methods are provided in Web Appendix C.

Table 4 exhibits the misclassification rate of MTR selection across these 10 scenarios. Our method might be conservative, as false negative rates are relatively high compared to false positive rates. However, our scheme performs reasonably well to control false positive rates in most of the scenarios.

We also conduct a sensitivity analysis to examine our design under the different sets of parameter values for the prior distributions under scenario 1. We choose two diffused prior distributions for parameters α and β and we also investigate the situation when the prior distributions for interaction parameters γ_1 and γ_2 are more informative. From Table 5a, the selection probabilities and number of patients allocated at each dose combination are quite similar under different sets of hyperparameters. We also investigate the operating characteristics across different prior distributions. Table 5b summarizes the percentage of observed toxicities, the percentage of patients treated at or below the MTDs, the sample size and the misspecification rate under each set of prior distribution. Again, our scheme is robust with respect to the prior specifications and there are only slight variations in terms of operating characteristics. Simulation study is also conducted to study the operating characteristics

for dosing individuals at synergy or antagonism regions of the dose space. The simulation results (Web Appendix C) demonstrate that our method can correctly identify the true synergy or antagonism with a high percentage in general. Although the percentages at some dose combinations under scenarios 1 and 2 are only around 50%, it is reasonable given that they are on the boundary between synergy and antagonism.

5. DISCUSSION

We have proposed a model-based Bayesian adaptive method for drug combination trials without assuming that toxicity monotonically increases with the dose, an issue which has been neglected by most studies that only concern traditional cytotoxic drugs. With the recent development of oncology drugs, the combination therapy has started to focus on molecularly-targeted therapies, vaccines, and immunotherapy. If either agent is not cytotoxic, Thall et al. [40] suggested that the method must account for the possibility that the joint toxicity probability may not increase in doses of each drug. Our method is developed by acknowledging that the interaction of two drugs may exhibit additive, antagonistic or synergistic behavior when they are administered together. Many existing toxicity response model in two-dimensional dose finding methods require the constant

Table 3. Percentage of MTR selection and number of patients treated at each dose combination under scenarios 5–10; the target MTR combinations are in boldface

		Drug A									
		Percentage of MTR Selection					Number of patients Allocation				
Dose Level		1	2	3	4	5	1	2	3	4	5
		Scenario 5									
	4	38.8	8.1	5.5	4.3		1.26	0.46	0.47	0.25	
	3	96.3	43.1	17.8	12.3		5.24	0.81	1.66	0.17	
	2	99.9	83.0	35.6	18.0		3.84	9.01	0.23	0.69	
	1	99.9	98.1	70.9	37.2		3.24	0.60	1.12	0.41	
		Scenario 6									
	4	45.8	11.2	7.1	4.8		1.57	0.69	0.42	0.24	
	3	96.5	45.0	15.2	9.6		5.17	1.22	1.42	0.10	
	2	99.9	80.5	28.6	13.1		3.94	8.73	0.14	0.48	
	1	99.9	98.1	63.4	27.1		3.32	0.63	0.94	0.24	
		Scenario 7									
	3	47.5	34.5	9.8	2.2	1.0	2.26	4.62	1.29	0.23	0.03
	2	85.8	26.6	4.8	1.8	1.4	3.84	1.30	0.46	0.16	0.04
Drug B	1	99.9	99.9	89.4	45.0	19.9	3.09	0.83	1.86	1.20	0.60
		Scenario 8									
	3	11.1	5.3	0.2	0.2	0.2	3.32	3.51	0.11	0.01	0.00
	2	75.5	9.1	0.9	0.3	0.4	4.92	0.34	0.06	0.06	0.01
	1	99.9	99.9	91.8	42.7	12.6	3.13	1.82	2.38	1.21	0.38
		Scenario 9									
	4	2.7	0.5	0.2	0.1	0.0	0.17	0.05	0.00	0.00	0.00
	3	9.6	0.9	0.1	0.0	0.1	1.12	0.02	0.02	0.00	0.00
	2	71.0	6.5	0.5	0.3	0.2	9.85	5.34	0.02	0.01	0.01
	1	99.9	79.2	10.1	2.2	0.7	5.24	4.54	1.66	0.19	0.02
		Scenario 10									
	4	10.1	2.8	0.6	0.3	0.1	0.57	0.17	0.02	0.01	0.00
	3	33.1	4.1	0.9	0.2	0.1	2.73	0.11	0.06	0.03	0.00
	2	92.8	23.8	3.3	1.2	0.6	11.25	5.71	0.12	0.04	0.02
	1	99.9	93.6	33.6	8.6	2.8	4.41	7.06	2.46	0.67	0.08

Table 4. False positive and false negative misclassification rate of MTR selection

		Scenario									
Misclassification Rate		1	2	3	4	5	6	7	8	9	10
False Positive		1.6	3.0	4.0	2.3	6.5	3.8	2.4	2.1	1.7	1.8
False Negative		47.4	50.6	15.0	52.5	14.8	19.7	24.4	12.1	2.5	11.2

Note: The false positive rate is the proportion of combination doses outside MTR that are incorrectly classified as MTR dose combinations. The false negative rate is the proportion of MTR dose combinations that are incorrectly classified as combination doses outside MTR.

drug-drug interaction function while some assume only synergistic effects between the combination agents. We demonstrate that the assumption of synergistic interaction is too restrictive and the joint toxicity probability may not be increasing in doses of both agents as compared to either one used alone. The monotonicity assumption may fail when synergy and antagonism are interspersed in different regions of combination space. Moreover, some of the existing models such as Thall et al. [40] are inadequate to describe the joint toxicity probabilities because their models do not satisfy the Bliss independence. For instance, when independence

happens, Thall et al.’s joint toxicity probability model cannot be expressed as $1 - \{1 - P(A)\}\{1 - P(B)\}$ in terms of the Bliss independence model. One important contribution of this article is that our approach naturally models the drug-drug interaction effects through a Bliss factorization, in which the proposed model can fully describe the varying interaction effect of the combined drugs, as well as evaluate its corresponding joint toxicity profiles.

Our approach identifies a region which is bounded by a tolerable toxicity probability ϕ . Fang et al. [13] described a method for interaction analysis of the preclinical combi-

Table 5a. Sensitivity analysis: selection probabilities and number of patients treated at each dose combination under alternative prior specifications in scenario 1; the target MTR combinations are in boldface

Dose Level	Percentage of MTR Selection					Number of patients Allocation				
	1	2	3	4	5	1	2	3	4	5
Set 1: $\alpha, \beta \sim \text{Gamma}(2.5, 5); \gamma_1, \gamma_2 \sim N(0, 100)$										
5	8.9	4.3	3.1	3.6	7.0	0.30	0.15	0.03	0.02	0.18
4	13.8	4.9	3.8	8.4	8.3	0.60	0.12	0.04	0.32	0.11
3	34.7	12.1	11.3	9.4	8.5	1.56	0.07	0.78	0.04	0.23
2	84.4	37.2	20.7	13.9	13.0	4.67	1.50	0.07	0.07	0.39
1	99.9	97.4	70.0	42.0	28.4	3.78	4.77	2.19	1.11	0.50
Set 2: $\alpha, \beta \sim \text{Gamma}(5, 5); \gamma_1, \gamma_2 \sim N(0, 100)$										
5	7.0	9.1	9.1	8.6	21.7	0.04	0.33	0.12	0.05	0.61
4	6.9	7.7	7.1	21.0	25.1	0.03	0.54	0.04	0.87	0.34
3	7.6	6.7	17.7	23.5	27.1	1.18	0.01	1.34	0.03	0.59
2	52.0	27.9	25.8	28.8	29.2	3.68	1.30	0.01	0.89	0.61
1	99.9	86.7	48.9	32.7	27.4	3.78	3.76	1.24	0.09	0.09
Set 3: $\alpha, \beta \sim \text{Gamma}(5, 5); \gamma_1, \gamma_2 \sim N(0, 50)$										
5	9.4	12.8	12.0	13.8	20.6	0.00	0.10	0.25	0.06	0.58
4	9.3	10.8	13.1	18.2	21.1	0.00	0.55	0.01	0.87	0.19
3	11.5	9.3	13.9	18.4	20.2	1.05	0.02	1.17	0.00	0.32
2	59.6	26.6	22.6	19.3	17.6	4.07	1.91	0.00	0.55	0.19
1	100.0	92.2	43.3	22.2	15.9	4.23	4.15	0.86	0.05	0.00

Table 5b. Sensitive analysis: operating characteristics

Set	1	2	3
% of observed toxicities	19.9	20.2	19.4
% of patients given doses at or below the MTD	94.7	94.7	95.5
Sample size	23.6	21.6	21.2
Misclassification Rate			
False Positive	1.7	2.2	3.2
False Negative	47.8	47.6	49.9

nation studies. Based on the preclinical interaction data *in vivo* and *in vitro*, several dose combinations in the MTR may be recommended for consideration for further study. Our dose finding scheme is based on posterior distributions of both toxicity and interaction function outcomes. We construct an objective function to provide the acceptable balance between toxicity and interaction, thus the patients are assigned to the dose combinations that minimize the objective function. Our extensive simulation studies under various scenarios demonstrate that the proposed design performs satisfactorily with expected operating characteristics. The proposed method is also compared with existing methods where the toxicity surfaces are considered to be monotonically increasing. The proposed method demonstrates satisfactory performance in general.

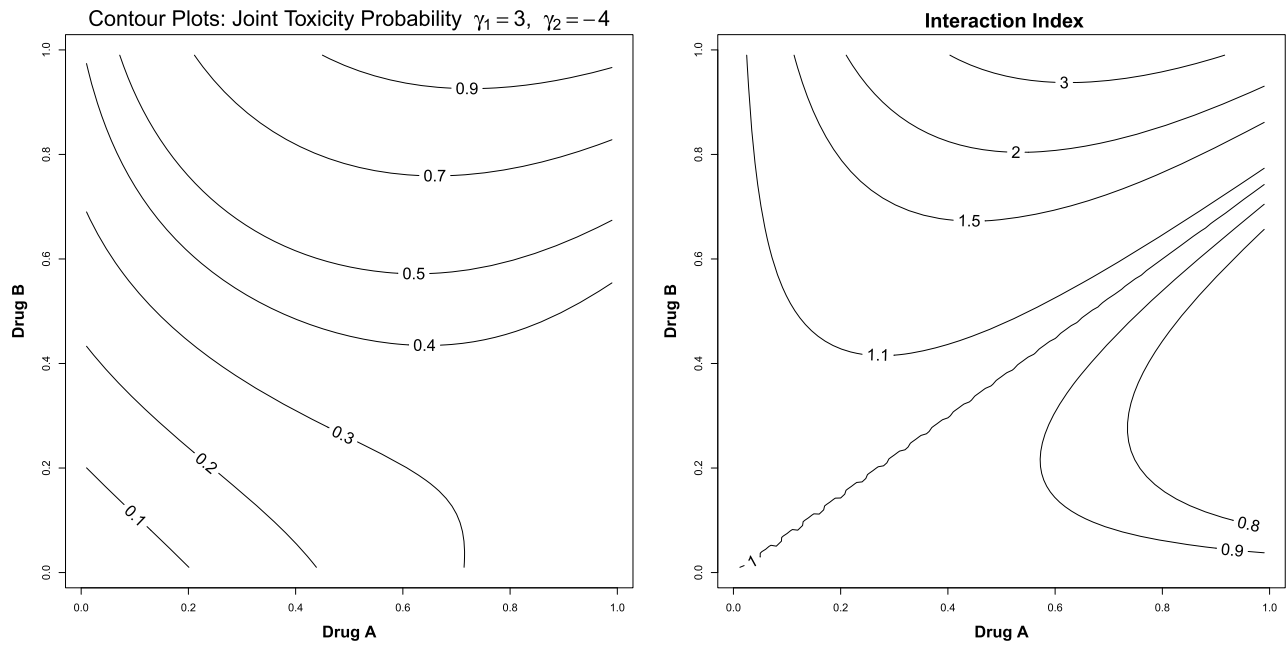
The proposed method does not assume any toxicity-dose relationship; the toxicity surface is captured and reshaped only in the search for MTR, making it feasible in actual clinical trial design. We have used a parametric function to detect drug interactions given the small sample nature of phase I design. When the patterns of drug interactions are complex, it would be worthwhile to consider semi-parametric extension to the current model to detect different patterns of drug interaction. Such extensions will be investigated in a separate report.

ACKNOWLEDGEMENTS

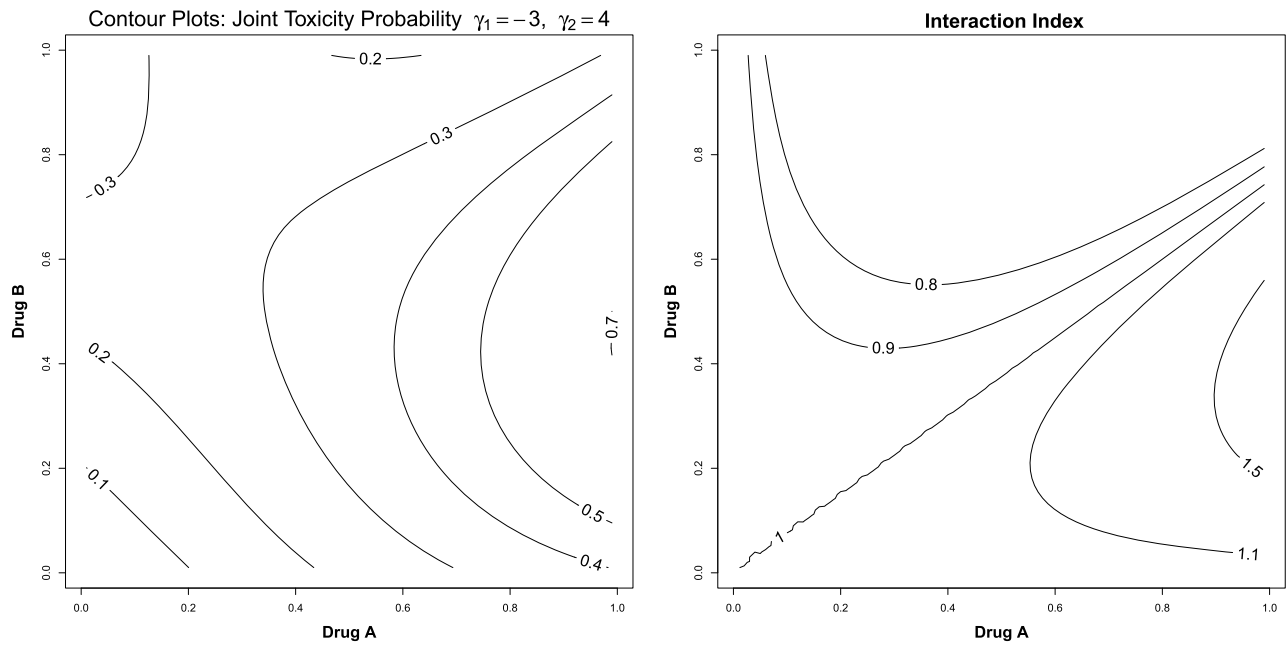
The research of Fang and Tan is partly supported by US National Cancer Institute award R01CA164717.

APPENDIX A. SIMULATION ON MODEL PERFORMANCE

We consider a simulation design that resembles the data for each scenario. Each simulated sample contains $n=75$ observations. We choose the dose level of agent A at (0.125, 0.25, 0.375, 0.5, 0.625) and agent B at (0.1, 0.3, 0.5, 0.7, 0.9). The cohort size is 3. The response is simulated by a binomial trial, given by $y \sim \text{Bin}(3, g(a_i, b_j, \theta))$. The simulation is repeated 1000 times for each scenario. For prior distributions, we take $\pi_1(\alpha) = \pi_1(\beta) = \text{Gamma}(25, 50)$, and non-informative priors $\pi_2(\gamma_1) = \pi_2(\gamma_2) = N(0, 100)$, respectively. We examine whether our model can correctly identify the interaction effect, synergy or antagonism, at each scenario in Figure A4.



Scenario 1



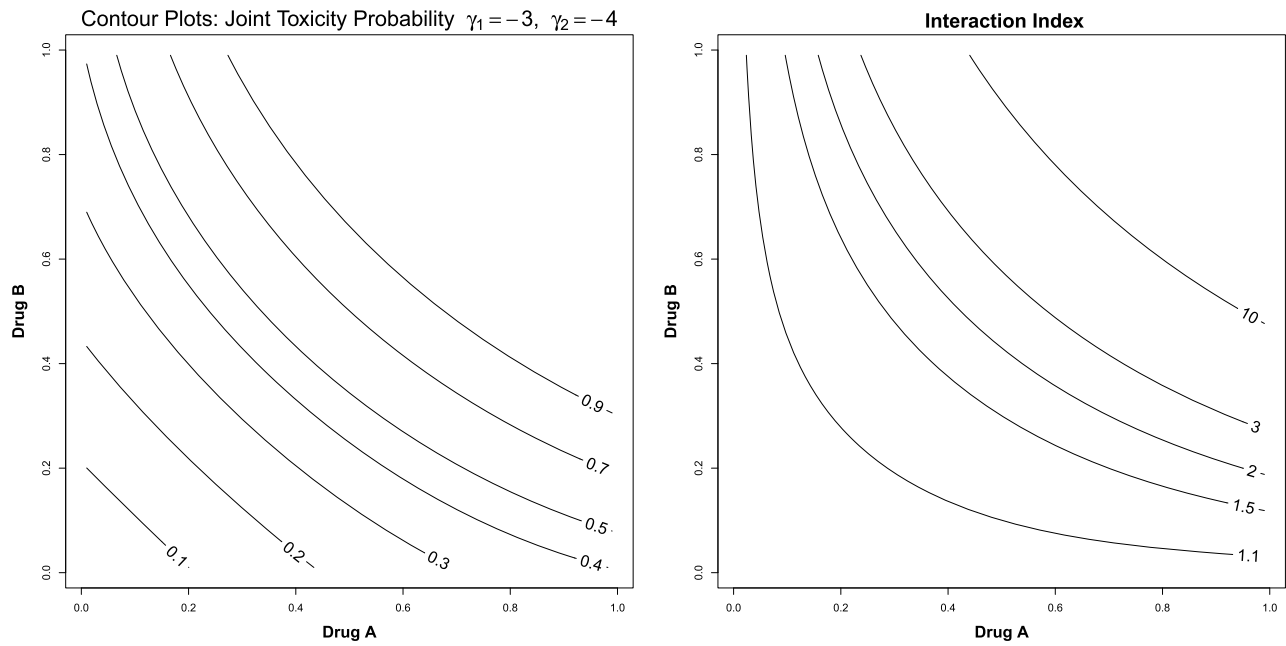
Scenario 2

Figure A3. Toxicity probability contour and interaction function contour under Scenarios 1–4.

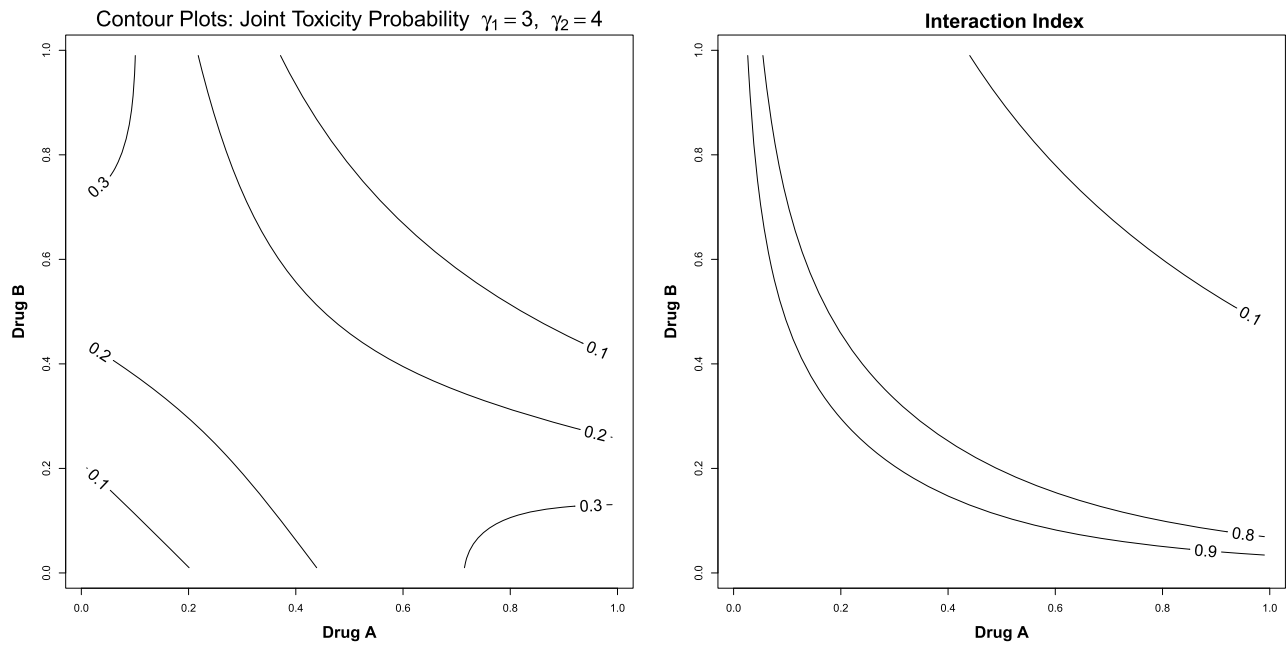
1st Scenario: the interaction effects between two combined agents change from synergy to antagonism. The contour plot of interaction function $f(\gamma_1, \gamma_2, d_A, d_B)$ is used to measure the degree of synergy or antagonism with the different dose combinations on the right panel that describes the interaction profile in the two-dimensional dose space. The straight line (marked as 1) represents the independence

of two agents. In the left-hand upper space, synergy is the dominant effect between two agents. Antagonism becomes dominant when the dose space moves to the right bottom.

2nd Scenario: the interaction effects between two combined agents change from antagonism to synergy. After the dose of agent A increases beyond a certain dose, the interaction effects between two combined agents change from



Scenario 3



Scenario 4

Figure A4. The last 4 figures of a continued Figure A3.

antagonism to synergy. We also illustrate this situation in contour plots. Compared to the interaction index in the 1st scenario, antagonism and synergy turn around in the dose space.

3rd Scenario: the interaction between two combined agents has increasing synergy effect. The model here shows that the combination therapies only have the synergy effect

on toxicity probabilities across all the dose combinations. With the dose level increases, the synergy effect also increases.

4th Scenario: the interaction between two combined agents has increasing antagonism effect. In contrast to the scenario above, the combination therapies only have the antagonism effect on toxicity probabilities across all the dose

combinations. The joint toxicity probability decreases as the dose increases, which means the antagonism effect is increasing.

We use “+” or “-” to denote the antagonism or synergy effect for each dose combination under each scenario as shown in Table A7. Table A8 demonstrates that our model can correctly identify the true synergy or antagonism with a high percentage in general. Although the percentages at some dose combinations under scenarios 1 and 2 are only around 50%, it is reasonable given that they are on the boundary between synergy and antagonism.

APPENDIX B. EVALUATION OF λ ON OBJECTIVE FUNCTION

To tune the value of the parameter λ in the objective function (14), we perform a simulation experiment. We first define a performance measure for the algorithm in terms of λ and glean knowledge about reasonable range of values for λ by studying the optimal values of the performance measure as a function of λ . There are three considerations that

are used in defining the performance measure and hence there are three ‘penalty’ terms that we want to minimize simultaneously for good performance. For a “good” value of λ , the toxicity probability surface should be well estimated and hence the performance measure includes the estimation error of the toxicity probability at the allocated doses. The second consideration is that the algorithm is expected to be heavily biased toward the antagonistic region. Hence we include the total amount of positive interaction (rescaled to the $[0, 1]$) at the allocated doses. The final consideration is the sample size. While it is intended that the algorithm explores the entire boundary of the MTR, it is also desirable that the determination of the boundary is done with the smallest possible sample. Thus we include the fraction of maximum allotted sample, n_{\max} spent before the algorithm terminates. To this end we define the following performance measure where a smaller value of the measure indicates better performance. Let $a = (0, \dots, A)$ and $b = (0, \dots, B)$. Suppose a trial stops at n_i th patient with a th dose of drug A and b th dose of drug B, we define the measure as:

$$M(\kappa, \lambda) = \kappa(AB)^{-1} \sum_{a=1}^A \sum_{b=1}^B [\hat{g}_{n_i}^\lambda(d_a, d_b) - g(d_a, d_b)]^2 + (1 - \kappa)n_i^{-1} \sum_{j=1}^{n_i} v(d_{a,j}^\lambda, d_{b,j}^\lambda) + n_i/n_{\max},$$

Table A7. Antagonism (+) or synergy effect (-) for each dose combination

		Drug A										
Dose Level		1	2	3	4	5	1	2	3	4	5	
		Scenario 1					Scenario 2					
Drug B	5	+	+	+	+	+	-	-	-	-	-	
	4	+	+	+	+	+	-	-	-	-	-	
	3	+	+	+	+	+	-	-	-	-	-	
	2	+	+	+	-	-	-	-	-	+	+	
	1	+	-	-	-	-	+	+	+	+	+	
			Scenario 3					Scenario 4				
	5	+	+	+	+	+	-	-	-	-	-	
	4	+	+	+	+	+	-	-	-	-	-	
	3	+	+	+	+	+	-	-	-	-	-	
	2	+	+	+	+	+	-	-	-	-	-	
1	+	+	+	+	+	-	-	-	-	-		

where \hat{g}_n^λ is the posterior estimate of the toxicity probability based on the n_i allocation and using v_λ and $(d_{a,j}^\lambda, d_{b,j}^\lambda)$ is the dose at which j th allocation occurred, i.e., the observed dose sequence. The values of $0 < \kappa \leq 1$ and $0 < \lambda \leq 1$ are also assumed. Now for each κ , define $\lambda(\kappa) = \underset{\lambda}{\operatorname{argmin}} M(\kappa, \lambda)$.

We conduct an empirical study to investigate the behavior of $\lambda(\kappa)$ so that if one specifies a measure with $\kappa = \kappa_0$ indicating the preference for having low positive interaction in the allocated dose combination. We construct four scenarios with different shapes of the toxicity probability surfaces as listed in Figure B5. Each simulated sample contains the

Table A8. Percentage of interaction function identifying the true synergy or antagonism at each dose combination

		Drug A										
Dose Level		1	2	3	4	5	1	2	3	4	5	
		Scenario 1					Scenario 2					
Drug B	5	94.9	96.4	97.8	98.3	95.5	94.0	96.6	98.5	99.0	99.0	
	4	95.8	97.6	98.6	95.6	73.8	94.2	97.4	98.9	98.0	91.0	
	3	97.3	99.0	94.8	63.8	42.8	94.7	98.4	96.4	79.6	66.5	
	2	98.6	88.4	48.1	67.1	75.0	97.7	90.8	60.1	49.8	52.7	
	1	49.5	72.1	76.2	78.3	80.1	59.0	63.0	66.0	66.6	66.4	
			Scenario 3					Scenario 4				
	5	96.9	99.5	99.0	99.0	99.0	94.4	98.8	99.8	99.0	99.0	
	4	98.4	99.0	99.0	99.0	99.0	95.4	99.5	99.0	99.0	99.0	
	3	99.5	99.0	99.0	99.0	99.7	97.2	99.0	99.0	99.0	99.5	
	2	99.0	99.0	99.9	97.2	93.1	99.8	99.0	99.0	95.9	93.5	
1	99.9	91.9	86.9	83.9	81.1	98.7	86.8	81.0	80.0	79.6		

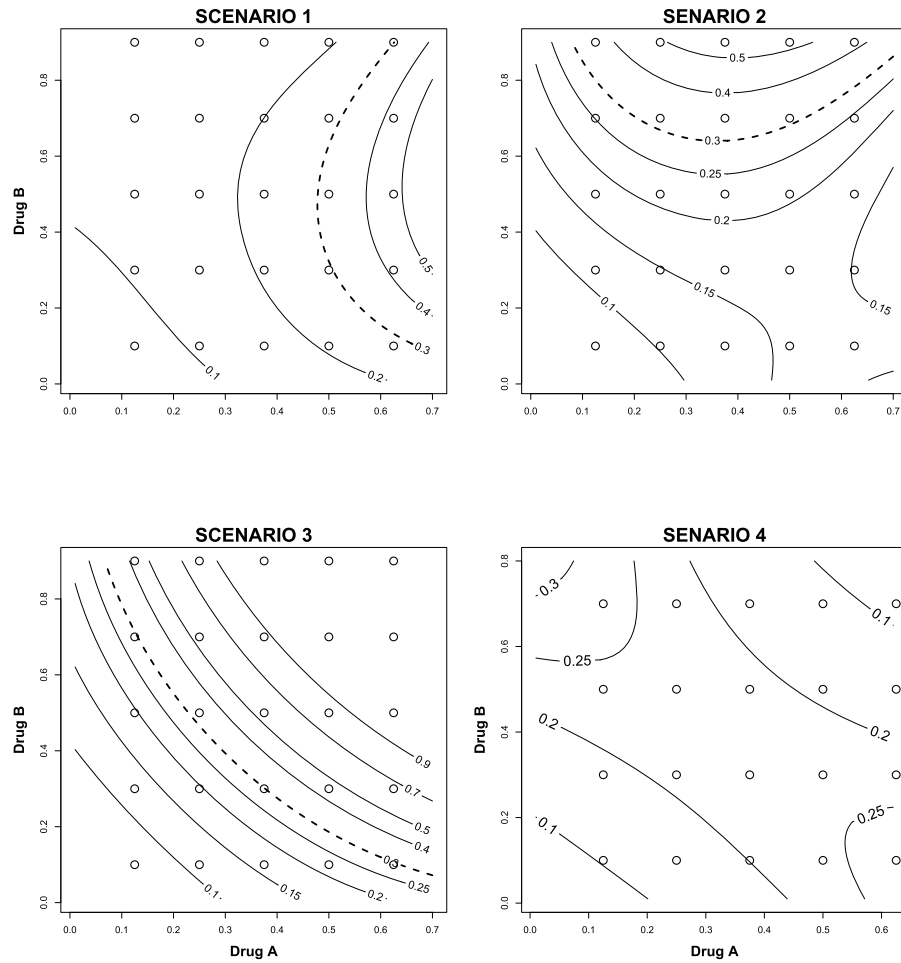


Figure B5. Scenarios for the probability of toxicity as a function of Drug A and B doses in combination trial. The target toxicity probability contour at 0.3 is considered to be the boundary of MTR region.

Table B9. $M(\kappa, \lambda)$ under a grid for both λ and κ in Scenario 1. $\lambda(\kappa)$ values are in boldface

	κ									
λ	0.1	0.2	0.3	0.4	0.5	0.6	0.7	0.8	0.9	1
0.1	0.8793	0.8387	0.7980	0.7573	0.7166	0.6759	0.6353	0.5946	0.5539	0.5132
0.2	0.8784	0.8380	0.7976	0.7571	0.7167	0.6762	0.6358	0.5954	0.5549	0.5145
0.3	0.8780	0.8370	0.7960	0.7550	0.7140	0.6730	0.6320	0.5910	0.5500	0.5090
0.4	0.8738	0.8328	0.7919	0.7510	0.7101	0.6692	0.6282	0.5873	0.5464	0.5055
0.5	0.8720	0.8314	0.7908	0.7502	0.7096	0.6689	0.6283	0.5877	0.5471	0.5065
0.6	0.8702	0.8293	0.7884	0.7475	0.7066	0.6656	0.6247	0.5838	0.5429	0.5020
0.7	0.8787	0.8381	0.7975	0.7570	0.7164	0.6759	0.6353	0.5947	0.5542	0.5136
0.8	0.8798	0.8392	0.7985	0.7579	0.7173	0.6766	0.6360	0.5954	0.5548	0.5141
0.9	0.8776	0.8366	0.7956	0.7546	0.7136	0.6726	0.6316	0.5907	0.5497	0.5087
1	0.8790	0.8383	0.7975	0.7567	0.7160	0.6752	0.6344	0.5936	0.5529	0.5121

maximum sample size $n_{max} = 60$. We choose the dose level of agent A at (0.125, 0.25, 0.375, 0.5, 0.625) and agent B at (0.1, 0.3, 0.5, 0.7, 0.9). The value of $M(\kappa, \lambda)$ is evaluated under a grid for both λ and κ . The simulation is repeated 2000 times by using the proposed algorithm for each scenario un-

der both λ values and κ values. For prior distributions, we take $\pi_1(\alpha) = \pi_1(\beta) = \text{Gamma}(25, 50)$, and non-informative priors $\pi_2(\gamma_1) = \pi_2(\gamma_2) = N(0, 100)$, respectively. Table B9–Table B12 report $M(\kappa, \lambda)$ across each grid combination of λ and κ . Through examination of these tables, it is clear

Table B10. $M(\kappa, \lambda)$ under a grid for both λ and κ in Scenario 2. $\lambda(\kappa)$ values are in boldface

λ	κ									
	0.1	0.2	0.3	0.4	0.5	0.6	0.7	0.8	0.9	1
0.1	0.8912	0.8528	0.8144	0.7759	0.7375	0.6991	0.6606	0.6222	0.5838	0.5454
0.2	0.8910	0.8526	0.8143	0.7760	0.7377	0.6994	0.6610	0.6227	0.5844	0.5461
0.3	0.8836	0.8455	0.8073	0.7692	0.7311	0.6929	0.6548	0.6166	0.5785	0.5404
0.4	0.8732	0.8348	0.7964	0.7580	0.7196	0.6811	0.6427	0.6043	0.5659	0.5275
0.5	0.8806	0.8425	0.8044	0.7663	0.7282	0.6901	0.6520	0.6140	0.5759	0.5378
0.6	0.8769	0.8383	0.7997	0.7611	0.7226	0.6840	0.6454	0.6068	0.5682	0.5296
0.7	0.8779	0.8395	0.8011	0.7627	0.7243	0.6859	0.6475	0.6091	0.5707	0.5323
0.8	0.8840	0.8456	0.8071	0.7686	0.7302	0.6917	0.6532	0.6147	0.5763	0.5378
0.9	0.8825	0.8438	0.8052	0.7665	0.7279	0.6892	0.6505	0.6119	0.5732	0.5346
1	0.8786	0.8401	0.8016	0.7631	0.7247	0.6862	0.6477	0.6092	0.5707	0.5323

Table B11. $M(\kappa, \lambda)$ under a grid for both λ and κ in Scenario 3. $\lambda(\kappa)$ values are in boldface

λ	κ									
	0.1	0.2	0.3	0.4	0.5	0.6	0.7	0.8	0.9	1
0.1	0.9463	0.8961	0.8460	0.7958	0.7456	0.6955	0.6453	0.5951	0.5449	0.4948
0.2	0.9412	0.8912	0.8412	0.7912	0.7412	0.6912	0.6412	0.5912	0.5412	0.4912
0.3	0.9349	0.8850	0.8350	0.7851	0.7352	0.6853	0.6354	0.5854	0.5355	0.4856
0.4	0.9300	0.8801	0.8302	0.7802	0.7303	0.6803	0.6304	0.5805	0.5305	0.4806
0.5	0.9314	0.8817	0.8321	0.7824	0.7327	0.6830	0.6333	0.5837	0.5340	0.4843
0.6	0.9180	0.8685	0.8189	0.7694	0.7199	0.6704	0.6209	0.5713	0.5218	0.4723
0.7	0.9285	0.8790	0.8294	0.7798	0.7302	0.6806	0.6311	0.5815	0.5319	0.4823
0.8	0.9321	0.8825	0.8330	0.7835	0.7340	0.6845	0.6349	0.5854	0.5359	0.4864
0.9	0.9205	0.8716	0.8227	0.7737	0.7248	0.6758	0.6269	0.5780	0.5290	0.4801
1	0.9261	0.8773	0.8284	0.7796	0.7308	0.6820	0.6332	0.5843	0.5355	0.4867

Table B12. $M(\kappa, \lambda)$ under a grid for both λ and κ in Scenario 4. $\lambda(\kappa)$ values are in boldface

λ	κ									
	0.1	0.2	0.3	0.4	0.5	0.6	0.7	0.8	0.9	1
0.1	0.8408	0.8122	0.7836	0.7550	0.7265	0.6979	0.6693	0.6407	0.6121	0.5836
0.2	0.8371	0.8084	0.7796	0.7509	0.7222	0.6934	0.6647	0.6360	0.6073	0.5785
0.3	0.8340	0.8055	0.7770	0.7484	0.7199	0.6913	0.6628	0.6343	0.6057	0.5772
0.4	0.8229	0.7937	0.7646	0.7354	0.7063	0.6771	0.6479	0.6188	0.5896	0.5605
0.5	0.8348	0.8063	0.7777	0.7491	0.7206	0.6920	0.6634	0.6348	0.6063	0.5777
0.6	0.8305	0.8011	0.7716	0.7422	0.7128	0.6833	0.6539	0.6244	0.5950	0.5656
0.7	0.8396	0.8102	0.7808	0.7515	0.7221	0.6927	0.6633	0.6339	0.6046	0.5752
0.8	0.8385	0.8088	0.7791	0.7494	0.7197	0.6899	0.6602	0.6305	0.6008	0.5711
0.9	0.8401	0.8100	0.7800	0.7499	0.7199	0.6898	0.6597	0.6297	0.5996	0.5696
1	0.8467	0.8167	0.7867	0.7567	0.7267	0.6967	0.6667	0.6367	0.6067	0.5767

that $\min_{\lambda} M(\kappa, \lambda)$ does exist for all the scenarios. We can see that $\arg\min_{\lambda} M(\kappa, \lambda)$ does not vary with κ values, whereas $\lambda(\kappa)$ changes slightly with different scenarios but centers around 0.5. We would consider using the objective function $U(d_A, d_B)$ with $\lambda = 0.5$ as a “base case” in our dose finding method. We have chosen a particular weight distribution across the three components of the performance measure, e.g. equal weights to the sample size fraction and the combined component of the estimation error and total positive interaction. Whether other weight distribution can change

the optimal range of values of λ will be investigated via further simulation. However, given that the choice of λ is insensitive to the choice of κ , we have refrained from such an elaborate investigation.

APPENDIX C. FURTHER DETAILS FOR SIMULATION STUDY

We examine the situations, in which the toxicity surfaces are monotonically increasing as MTDs are considered to be on the boundary of the MTRs. Table C13 reports the

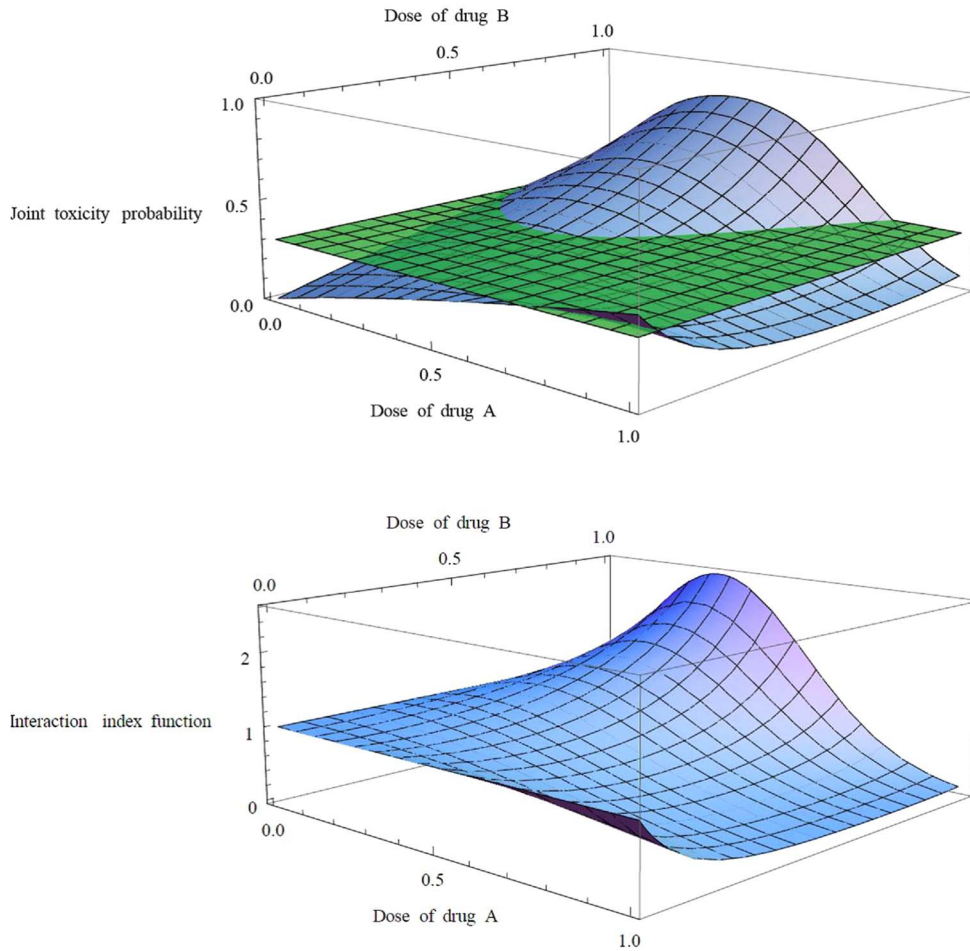


Figure C6. Toxicity probability surface and interaction function surface with a target toxicity probability 30% for the two-drug combination.

Table C13. Comparison with existing methodology

Method	Scenario					
	5	6	7	8	9	10
	% of observed toxicities					
New method	18.7	18.7	20.8	27.5	39.1	31.4
Yin and Yuan	27.9	27.7	28.1	29.1	36.9	35.2
POCRM	31.1	31.1	31.3	33.4	46	44
	% of patients given doses at or below the MTD					
New method	83.2	88.5	88.9	64.6	69.4	94.4
Yin and Yuan	68.7	75.3	74.7	71.1	65	77.5
POCRM	67	69	81	68	34	46
	Sample size					
New method	29.4	29.3	21.9	21.4	28.3	35.6
Yin and Yuan	56.9	56.7	56.9	56.8	57.7	58.7
POCRM	57	57	57	57	57	57

percentage of observed toxicities, the percentage of patients treated at or below the MTDs, and the sample size for the proposed method and for the POCRM (Wages et al., 2011) and for both designs of Yin and Yuan (2009a,b).

In Figure C6, we depict the joint toxicity probability surface and also the interaction surface in the two-dimensional dose region on the basis of a model (7) with parameters $(\alpha, \beta, \gamma_1, \gamma_2) = (0.5, 0.5, 8, -5.5)$. The interaction surface implies that synergy and antagonism may be interspersed in different regions of the drug combinations, which leads to a non-monotonically increasing toxicity probability surface. The exponent in the interaction function is a saddle like surface with negative curvature; however the interaction function itself under the exponential transformation can have both positive and negative curvature, thereby allowing for great flexibility. The horizontal surface in Figure C6 represents the situation of a target toxicity probability of 0.3.

We further conduct the simulation study to examine whether our method can correctly identify the interaction effect, synergy or antagonism of the dose combinations for scenario shown in Figure C6. Table C14 lists the interaction

Table C14. Interaction: antagonism (+) or synergy effect (-)

		Drug A				
Dose Level		1	2	3	4	5
Drug B	5	1.56 (-)	1.94 (-)	1.93 (-)	1.53 (-)	0.97 (+)
	4	1.28 (-)	1.38 (-)	1.25 (-)	0.95 (+)	0.61 (+)
	3	1.12 (-)	1.10 (-)	0.95 (+)	0.73 (+)	0.50 (+)
	2	1.03 (-)	0.97 (+)	0.86 (+)	0.70 (+)	0.53 (+)
	1	0.99 (+)	0.96 (+)	0.91 (+)	0.84 (+)	0.76 (+)

Table C15. Percentage of interaction function identifying the true synergy or antagonism

		Drug A				
Dose Level		1	2	3	4	5
Drug B	5	60.93	66.01	65.88	60.53	49.30
	4	56.20	58.02	55.56	48.69	37.68
	3	52.73	52.34	48.83	42.25	33.11
	2	50.61	49.34	46.21	41.28	34.79
	1	49.86	49.09	47.70	45.70	43.09

for each dose combination. We use “+” or “-” to denote the antagonism (+) or synergy effect (-). Table C15 reports the selection probabilities for the true synergy or antagonism.

Received 25 August 2016

REFERENCES

- ABDELBASIT, K. M. and PLACKETT, R. L. Experimental design for joint action. *Biometrics*, pages 171–179, 1982.
- ANSCHER, M. S., MARKS, L. B., SHAFMAN, T. D., CLOUGH, R., HUANG, H., TISCH, A., MUNLEY, M., HERNDON, J. E., GARST, J., CRAWFORD, J., et al. Using plasma transforming growth factor beta-1 during radiotherapy to select patients for dose escalation. *Journal of clinical oncology*, 19(17):3758–3765, 2001.
- ASHFORD, J. R. General models for the joint action of mixtures of drugs. *Biometrics*, pages 457–474, 1981. [MR0676169](#)
- BENTZEN, S. M. and TROTTI, A. Evaluation of early and late toxicities in chemoradiation trials. *Journal of clinical oncology*, 25(26):4096–4103, 2007.
- BERENBAUM, M. C. What is synergy? *Pharmacological Reviews*, 41(2):93–141, 1989.
- BERENSON, J. R., YELIN, O., PATEL, R., DUVIVIER, H., NASSIR, Y., MAPES, R., ABAYA, C. D., and SWIFT, R. A. A phase i study of samarium lexidronam/bortezomib combination therapy for the treatment of relapsed or refractory multiple myeloma. *Clinical Cancer Research*, 15(3):1069–1075, 2009.
- BERRY, S. M., CARLIN, B. P., LEE, J. J., and MULLER, P. *Bayesian adaptive methods for clinical trials*. CRC press, 2010. [MR2723582](#)
- BRAUN, T. M. The bivariate continual reassessment method: extending the crm to phase i trials of two competing outcomes. *Controlled clinical trials*, 23(3):240–256, 2002.
- CHEUNG, Y. K. and CHAPPELL, R. Sequential designs for phase i clinical trials with late-onset toxicities. *Biometrics*, 56(4):1177–1182, 2000.
- COIA, L. R., MYERSON, R. J., and TEPPER, J. E. Late effects of radiation therapy on the gastrointestinal tract. *International Journal of Radiation Oncology* Biology* Physics*, 31(5):1213–1236, 1995.
- COOPER, J. S., FU, K., MARKS, J., and SILVERMAN, S. Late effects of radiation therapy in the head and neck region. *International Journal of Radiation Oncology* Biology* Physics*, 31(5):1141–1164, 1995.
- DURRANT, G. B. and SKINNER, C. Using data augmentation to correct for non-ignorable non-response when surrogate data are available: an application to the distribution of hourly pay. *Journal of the Royal Statistical Society: Series A (Statistics in Society)*, 169(3):605–623, 2006.
- FANG, H.-B., ROSS, D. D., SAUSVILLE, E., and TAN, M. Experimental design and interaction analysis of combination studies of drugs with log-linear dose responses. *Statistics in medicine*, 27(16):3071–3083, 2008.
- FARIES, D. Practical modifications of the continual reassessment method for phase i cancer clinical trials. *Journal of biopharmaceutical statistics*, 4(2):147–164, 1994.
- FITZGERALD, J. R., FOSTER, T. J., and COX, D. The interaction of bacterial pathogens with platelets. *Nature Reviews Microbiology*, 4(6):445–457, 2006.
- GANDHI, L., BAHLEDA, R., TOLANEY, S. M., KWAK, E. L., CLEARY, J. M., PANDYA, S. S., HOLLEBECQUE, A., ABBAS, R., ANANTHAKRISHNAN, R., BERKENBLIT, A., et al. Phase i study of neratinib in combination with temsirolimus in patients with human epidermal growth factor receptor 2-dependent and other solid tumors. *Journal of Clinical Oncology*, 32(2):68–75, 2014.
- GASPARINI, M. General classes of multiple binary regression models in dose finding problems for combination therapies. *Journal of the Royal Statistical Society: Series C (Applied Statistics)*, 62(1):115–133, 2013.
- GILKS, W. R., BEST, N. G., and TAN, K. K. C. Adaptive rejection metropolis sampling within gibbs sampling. *Applied Statistics*, pages 455–472, 1995.
- GOODMAN, S. N., ZAHURAK, M. L., and PIANTADOSI, S. Some practical improvements in the continual reassessment method for phase i studies. *Statistics in medicine*, 14(11):1149–1161, 1995.
- IBRAHIM, J. G., CHEN, M.-H., LIPSITZ, S. R., and HERRING, A. H. Missing-data methods for generalized linear models: A comparative review. *Journal of the American Statistical Association*, 100(469):332–346, 2005. [MR2166072](#)
- KORN, E. L. and SIMON, R. Using the tolerable-dose diagram in the design of phase i combination chemotherapy trials. *Journal of Clinical Oncology*, 11(4):794–801, 1993.
- KORN, E. L., MIDTHUNE, D., CHEN, T. T., RUBINSTEIN, L. V., CHRISTIAN, M. C., and SIMON, R. M. A comparison of two phase i trial designs. *Statistics in medicine*, 13(18):1799–1806, 1994.
- LIU, S., NING, J., et al. A bayesian dose-finding design for drug combination trials with delayed toxicities. *Bayesian Analysis*, 8(3):703–722, 2013. [MR3102231](#)
- LIU, S., YIN, G., YUAN, Y., et al. Bayesian data augmentation dose finding with continual reassessment method and delayed toxicity. *The annals of applied statistics*, 7(4):2138–2156, 2013. [MR3161716](#)
- MACCULLAGH, P. and NELDER, J. A. Generalized linear models. 1989.
- MANDREKAR, S. J. Dose-finding trial designs for combination therapies in oncology. *Journal of Clinical Oncology*, 32(2):65–67, 2014.
- MÖLLER, S. An extension of the continual reassessment methods using a preliminary up-and-down design in a dose finding study in cancer patients, in order to investigate a greater range of doses. *Statistics in medicine*, 14(9):911–922, 1995.
- MULER, J. H., MCGINN, C. J., NORMOLLE, D., LAWRENCE, T., BROWN, D., HEJNA, G., and ZALUPSKI, M. M. Phase i trial using a time-to-event continual reassessment strategy for dose escalation of cisplatin combined with gemcitabine and radiation therapy in pancreatic cancer. *Journal of clinical oncology*, 22(2):238–243, 2004.
- NELDER, J. A. and MEAD, R. A simplex method for function minimization. *The computer journal*, 7(4):308–313, 1965.

- [30] O'QUIGLEY, J. and SHEN, L. Z. Continual reassessment method: a likelihood approach. *Biometrics*, pages 673–684, 1996.
- [31] O'QUIGLEY, J., PEPE, M., and FISHER, L. Continual reassessment method: a practical design for phase I clinical trials in cancer. *Biometrics*, pages 33–48, 1990.
- [32] ROSENBERGER, W. F. and HAINES, L. M. Competing designs for phase I clinical trials: a review. *Statistics in Medicine*, 21(18): 2757–2770, 2002.
- [33] SIMON, R. and KORN, E. L. Selecting drug combinations based on total equivalent dose (dose intensity). *Journal of the National Cancer Institute*, 82(18):1469–1476, 1990.
- [34] STORER, B. E. Design and analysis of phase I clinical trials. *Biometrics*, pages 925–937, 1989. [MR1029610](#)
- [35] SWEETING, M. J. and MANDER, A. P. Escalation strategies for combination therapy phase I trials. *Pharmaceutical statistics*, 11(3):258–266, 2012.
- [36] TAN, M., FANG, H.-B., TIAN, G.-L., and HOUGHTON, P. J. Experimental design and sample size determination for testing synergism in drug combination studies based on uniform measures. *Statistics in medicine*, 22(13):2091–2100, 2003.
- [37] TAN, M. T. and XIONG, X. A flexible multi-stage design for phase II oncology trials. *Pharmaceutical statistics*, 10(4):369–373, 2011.
- [38] TANNER, M. A. and WONG, W. H. The calculation of posterior distributions by data augmentation. *Journal of the American statistical Association*, 82(398):528–540, 1987.
- [39] THALL, P. F. and COOK, J. D. Dose-finding based on efficacy–toxicity trade-offs. *Biometrics*, 60(3):684–693, 2004. [MR2089444](#)
- [40] THALL, P. F., MILLIKAN, R. E., MUELLER, P., and LEE, S.-J. Dose-finding with two agents in phase I oncology trials. *Biometrics*, 59(3):487–496, 2003.
- [41] VARGAS, C., MARTINEZ, A., KESTIN, L. L., YAN, D., GRILLS, I., BRABBINS, D. S., LOCKMAN, D. M., LIANG, J., GUSTAFSON, G. S., CHEN, P. Y., et al. Dose-volume analysis of predictors for chronic rectal toxicity after treatment of prostate cancer with adaptive image-guided radiotherapy. *International Journal of Radiation Oncology* Biology* Physics*, 62(5):1297–1308, 2005.
- [42] WAGES, N. A., CONAWAY, M. R., and O'QUIGLEY, J. Continual reassessment method for partial ordering. *Biometrics*, 67(4):1555–1563, 2011. [MR2872406](#)
- [43] WAGES, N. A., CONAWAY, M. R., and O'QUIGLEY, J. Using the time-to-event continual reassessment method in the presence of partial orders. *Statistics in medicine*, 32(1):131–141, 2013.
- [44] WANG, K. and IVANOVA, A. Two-dimensional dose finding in discrete dose space. *Biometrics*, 61(1):217–222, 2005.
- [45] YIN, G. and YUAN, Y. Bayesian dose finding in oncology for drug combinations by copula regression. *Journal of the Royal Statistical Society: Series C (Applied Statistics)*, 58(2):211–224, 2009. [MR2649671](#)
- [46] YIN, G. and YUAN, Y. A latent contingency table approach to dose finding for combinations of two agents. *Biometrics*, 65(3): 866–875, 2009.
- [47] YUAN, Y. and YIN, G. Sequential continual reassessment method for two-dimensional dose finding. *Statistics in medicine*, 27(27): 5664–5678, 2008.
- [48] YUAN, Y. and YIN, G. Robust em continual reassessment method in oncology dose finding. *Journal of the American Statistical Association*, 106(495), 2011.

Yang Yang

Department of Mathematics and Statistics
University of Maryland Baltimore County
Baltimore, MD
U.S.A.

E-mail address: yang10@umbc.edu

Hong-Bin Fang

Department of Biostatistics, Bioinformatics
and Biomathematics
Georgetown University
Washington, D.C.
U.S.A.

E-mail address: hf183@georgetown.edu

Anindya Roy

Department of Mathematics and Statistics
University of Maryland Baltimore County
Baltimore, MD
U.S.A.

E-mail address: anindya@umbc.edu

Ming Tan

Department of Biostatistics, Bioinformatics
and Biomathematics
Georgetown University
Washington, D.C.
U.S.A.

E-mail address: mtt34@georgetown.edu